

Imaging-XPS/Raman investigation on the carbonization of polyimide after irradiation at 308 nm

T. Lippert*, E. Ortelli, J.-C. Panitz, F. Raimondi, J. Wambach, J. Wei, A. Wokaun

Paul Scherrer Institut, CH-5232 Villigen PSI, Switzerland

Received: 21 July 1999/Accepted: 1 September 1999/Published online: 22 December 1999

Abstract. The laser ablation of polyimide was studied using 308 nm laser irradiation $\leq 225 \text{ mJ cm}^{-2}$. Confocal Raman microscopy revealed the deposition of carbon surrounding the ablation crater, which consists of amorphous carbon with some crystalline features. Inside the crater, graphitic material was detected on top of the cones, very similar to the material from cw-Ar⁺ ion laser irradiation. FT-Raman measurements reveal the presence of intermediates of the polyimide decomposition. Imaging-X-ray photoelectron spectroscopy confirmed the deposition of carbon material surrounding the ablation crater and showed that the oxygen and nitrogen contents of the remaining material decrease.

PACS: 79.20.D; 61.80.B; 61.82.P

There have been many reports about the laser ablation of polymers over the last 17 years. Polyimide (PI) is probably the polymer studied in most detail [1–3]. The reasons for the interest in PI are numerous, including industrial applications such as via holes in multichip modules [4] and the fabrication of the nozzles in inkjet printer heads [5]. Polyimide shows a broad UV absorption band that allows high-quality structuring with all common excimer wavelengths (193, 248, 308 and 351 nm) [6]. It is generally agreed that the mechanism of ablation is mainly photothermal, with additional photochemical features especially at 193 nm irradiation [7]. The existence of a sharp ablation threshold and Arrhenius tails was explained recently by Arnold and Bityurin [8] using a model combining photochemical volume with thermal surface features. Another effect of UV irradiation of polymers is the possibility of changing physical properties of the polymer. It has been reported that it is possible to induce electrical conductivity (increase of up to 12 orders of magnitude) into polyimide by laser irradiation [9, 10]. The resulting conductivity was assigned to carbonization of the surface [11]. Most

studies used KrF (248 nm) excimer laser irradiation, with fluences below 1 J cm^{-2} or the scanning beam of a cw-Ar⁺ laser with wavelengths from 275 to 380 nm [12, 13]. For the cw-irradiated PI it has been suggested that the conducting material has a completely different microstructure, namely highly crystalline material together with nanosized crystallites [11]. The excimer laser treatment at 248 nm did not cause complete graphitization of the polymer as reported for the pyrolyzation [14]. Analysis of the irradiated (193 and 248 nm), conducting PI using X-ray photoelectron spectroscopy (XPS) revealed an increase of the atomic percentage of carbon [15, 16].

For a better understanding of the carbonization/ablation mechanism of PI after 308 nm irradiation we decided to combine two analytical techniques with lateral resolution, namely imaging-XPS and Raman spectroscopy. Moreover, FT-Raman spectroscopy was used in order to exploit its capability to overcome the inherent fluorescence problem of polymer samples in Raman spectroscopy.

1 Experimental

The polyimide (KaptonTM) was supplied by Goodfellow. For the irradiation an XeCl-excimer laser (Lambda Physik Compex 205) emitting at 308 nm was used. XPS spectra were recorded with an ESCALAB 220I XL (VG Scientific) photoelectron spectrometer, using non-monochromatized Mg K_{α} radiation at a source power of 300 W. FT-Raman measurements were performed with a BRUKER FRA106/S FT-RAMAN using a liquid nitrogen-cooled germanium detector and a 1064 nm Nd:YAG laser. All spectra were collected with an accumulation of 1024 scans with a resolution of 4 cm^{-1} . Raman spectra were measured with a Raman-microscope (Labram, DILOR) equipped with an objective (100× magnification) and a thermoelectrically cooled charge-coupled device detector. Spectra were acquired in the range 250–4000 cm^{-1} with a Kr⁺ ion laser operating at 530.9 nm. Laser power was adjusted to 150 μW (0.375 W cm^{-2}) at the sample, in order to avoid disruption of the sample. Higher laser power resulted in removal of the thin carbon layer, which could be observed with the video microscope.

*Corresponding author.
(Fax: +41-56/310-2199, E-mail: lippert@psi.ch)

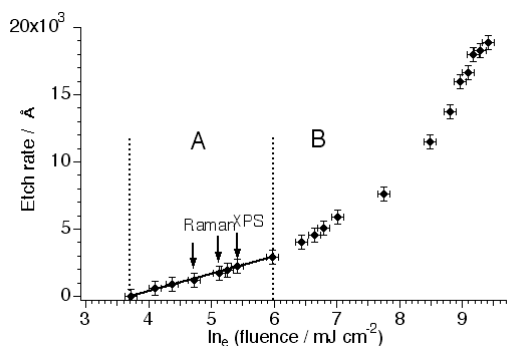


Fig. 1. Ablation depths vs. \ln_e relationship for 308 nm laser irradiation of a polyimide film. A denotes the linear region of the etch plot, yielding a threshold fluence of 40 mJ cm^{-2} and effective absorption coefficient of $78\,000 \pm 2\,000 \text{ cm}^{-1}$. Arrows mark the applied fluences for the Raman and XPS analysis

2 Results and discussion

The etch rate vs. the laser fluence (shown in Fig. 1) of PI irradiated at 308 nm reveals clearly two different areas: in the low fluence range (A), the etch depth depends linearly on \ln_e (fluence), with a slope close to the prediction by Beer's law. The linear fit in Fig. 1 yields an effective absorption coefficient, α , of $78\,000 \pm 2\,000 \text{ cm}^{-1}$ while a value of $86\,000\text{--}100\,000 \text{ cm}^{-1}$ was reported [6, 8] for the linear absorption coefficient. In the high fluence range (B), the etch depth deviates from Beer's law.

In Fig. 2 the FT-Raman spectrum of the untreated polyimide film is shown together with the spectrum of a film irradiated with 500 pulses and a fluence of 40 mJ cm^{-2} . Several characteristic bands of polyimide are present [17, 18]. In the spectra of the irradiated sample, which is multiplied by a factor of 8, a new broad band located at 1280 cm^{-1} is detected. This band can be assigned to various decomposition intermediates, which are the subject of detailed study in our group. Because of the strong absorption of carbon in the near infrared (1064 nm of the laser in the FT-Raman instrument) it was not possible to obtain spectra of the carbonized surface. The black layer disappeared during the measurement.

Thus Raman microscopy with a laser emitting in the visible was chosen to study the irradiated surface of the polyimide. For the Raman microscopy study fluences in the linear range of the ablation plot were chosen, because of the clearly observable optical blackening of the surface. Raman spectra

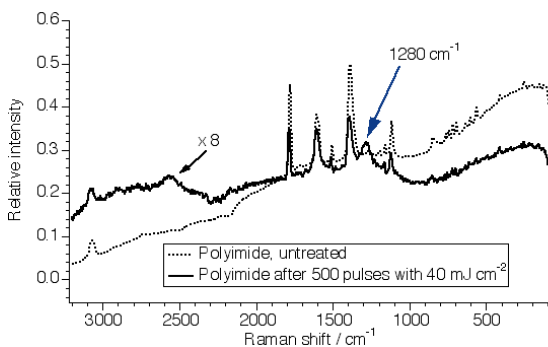


Fig. 2. FT-Raman spectra of untreated polyimide and after irradiation with 500 pulses at 40 mJ cm^{-2} . The irradiated spectrum is multiplied by 8

were recorded inside the ablation craters and outside. Bands not corresponding to PI could be recorded outside the crater only after irradiation with about 200 pulses at 120 mJ cm^{-2} . The spectra consist of two lines at around 1360 (D-band) and 1580 cm^{-1} (G-band). This is characteristic of carbon with crystalline features [19]. Amorphous carbon would only show a broad band in this region [20]. In Fig. 3 (top) the Raman mapping of the carbon bands (shown in Fig. 3, bottom) is shown. The three squares inside the image (from left to right) represent the top three spectra in Fig. 3 (bottom). The ablation crater is located just outside the bottom left corner. The clear decrease of the carbon intensity corresponds to a decreasing amount of redeposited carbon species, within the penetration depths of the Raman laser into the carbon ($\approx 200 \text{ nm}$). The D- and G-bands are clearly recognizable, suggesting an at least partly crystalline structure. We also observe (not shown) the development of cone-like structures in the ablation crater. The spectra in Fig. 4 show the Raman spectra of PI irradiated with 800 pulses at 160 mJ cm^{-2} . The spectrum inside the crater (Fig. 4, lowest trace) is taken at the top of one of the cones and shows the D and G band and an additional band at 2720 cm^{-1} , which corresponds to the two-phonon band of the D band, and is a typical sign of graphitic carbon [20]. Figure 4 also reveals that the amount of graphitic material varies inside the crater and that the redeposited material outside has a more amorphous structure. The spectra taken inside the crater suggest that

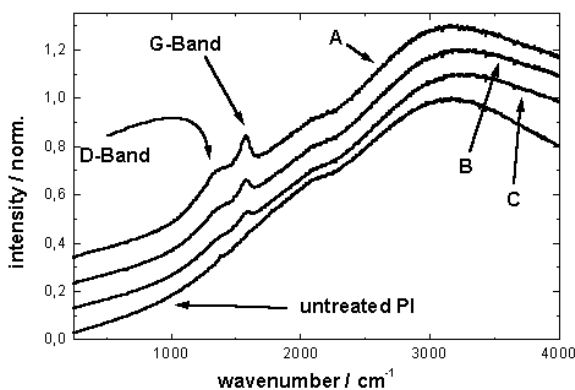
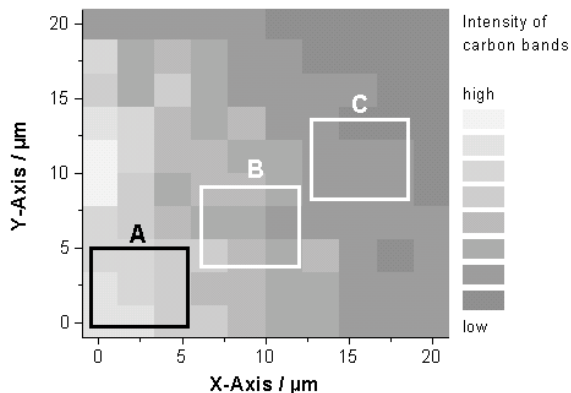


Fig. 3. top: Raman mapping of the carbon bands (intensities of the D and G band). The polyimide was irradiated with 200 pulses at 120 mJ cm^{-2} . The edge of the ablation crater is just outside of the bottom left corner. Bottom: Raman spectra corresponding to the three squares in the mapping picture (left to right corresponds to the top to bottom spectra)

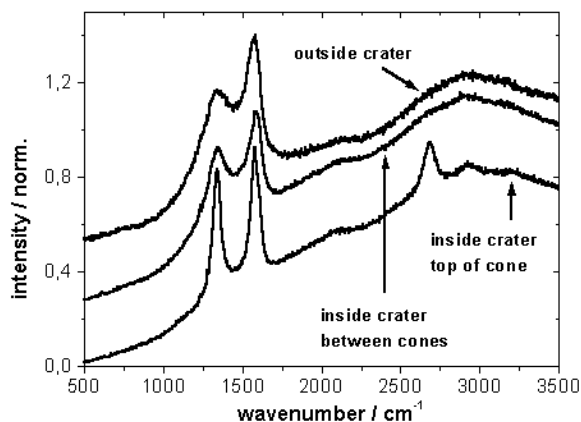


Fig. 4. Raman spectra inside and outside a crater in polyimide irradiated with 800 pulses at 160 mJ cm^{-2}

at least the chemical structure (graphitic) is very similar to the material detected after irradiation with the cw-Ar⁺ ion laser, even if the morphology is quite different.

The lateral resolution of the Raman microscope is $2 \mu\text{m}$, while the average size of the cone tops is $\approx 1\text{--}2 \mu\text{m}$. Therefore it was possible to distinguish between the cone tops and the material between the cones.

A complementary technique to Raman microscopy is Imaging-XPS, which was used with a lower lateral resolution ($15 \mu\text{m}$), but is more sensitive due to the smaller penetration depths ($\approx 20 \text{ nm}$). The small spot analysis ($150 \mu\text{m}^2$) inside the crater of the PI irradiated with 10 pulses at 225 mJ cm^{-2} revealed an increase (from 77% for the original material to 90% after irradiation) of the carbon atomic percentage with a corresponding decrease in the nitrogen and oxygen content. In Fig. 5 (top) the image of the O 1s peak is shown for irradiation with 10 pulses at 225 mJ cm^{-2} . Dark colors denote a decrease in the atomic percentage. The ablation crater with a diameter of 300 microns is clearly recognizable. The surrounding ring, with a width of about 600 microns, shows a low oxygen content, due to the coverage of this area by deposited carbon. The line scan (Fig. 5, bottom) reveals that inside the crater the oxygen content is reduced too, compared with the original material. Using standard data processing (peak-background/peak+background) excludes the influence of surface roughening. The results of the small spot analysis also revealed a reduction of the O content, suggesting that the lower O content inside the crater in the line scan in Fig. 5 is real and not an artifact of surface roughening. The relatively higher oxygen content in the crater, compared with the surrounding ring, can be explained by the cone structures in the ablation crater, which probably also give rise to detection of non-carbonized PI, or more probably by the continuing ablation of the carbon material in the crater upon successive pulses. The diameter of the centric deposited material increases with increasing fluence and pulse numbers (up to several mm).

3 Conclusion

We have studied the ablation and carbonization of polyimide using 308 nm laser irradiation with two techniques with lateral resolution. Raman microscopy reveals the deposition of

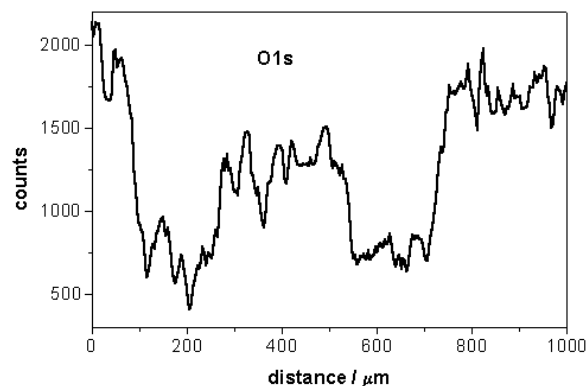
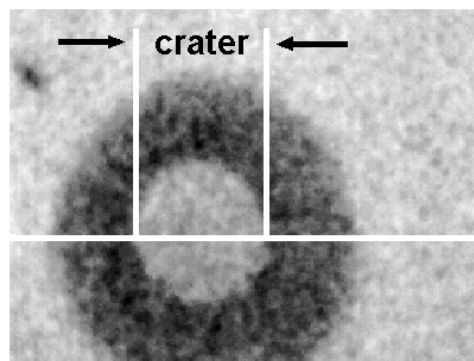


Fig. 5. *top*: XPS image (256×256 pixels; CRR = 4, background corrected) of the O 1s peak of a crater irradiated with 10 pulses and a fluence of 225 mJ cm^{-2} . *Bottom*: the line in the image represents the position of the corresponding line scan

carbon material surrounding the crater after irradiation with fluences around 100 mJ cm^{-2} . The material is amorphous carbon with partly crystalline structure. The decomposition of polyimide inside the ablation crater yields at least some graphitic carbon, but the coverage is not complete or very thick, as demonstrated with imaging XPS. The graphitic material is very similar to the material received after irradiation with a cw-Ar⁺ ion laser, even if the morphology is quite different.

Acknowledgements. This work was financially supported by the Swiss National Science Foundation.

References

1. R. Srinivasan, B. Brannen: *Chem. Rev.* **89**, 1303 (1989)
2. S. Lazare, V. Granier: *Laser Chem.* **10**, 25 (1989)
3. P.E. Dyer: In *Photochemical Processing of Electronic Materials*, ed. by I.A. Boyd (Academic Press, London 1992) pp. 359–385
4. J.R. Lankard Jr., G. Wolbold: *Appl. Phys. A* **54**, 355 (1992)
5. E.g. H. Aoki: US Patent 5736999, issued 04/1998
6. J.H. Brannon, J.R. Lankard, A.I. Baise, F. Burns, J. Kaufman: *J. Appl. Phys.* **58**, 2036 (1985)
7. S. Küper, J. Brannon, K. Brannon: *Appl. Phys. A* **56**, 43 (1993)
8. N. Arnold, N. Bityurin: *Appl. Phys. A* **68**, 615 (1999)
9. M. Schumann, R. Sauerbrey, M.C. Smayling: *Appl. Phys. Lett.* **58**, 428 (1991)

10. Z. Ball, R. Sauerbrey: *Appl. Phys. Lett.* **65**, 391 (1994)
11. Z. Ball, T. Feurer, D.L. Callahan, R. Sauerbrey: *Appl. Phys. A* **62**, 203 (1996)
12. T. Feurer, R. Sauerbrey, M.C. Smayling, B.J. Story: *Appl. Phys. A* **56**, 275 (1993)
13. R. Srinivasan, R.R. Hall, W.D. Wilson, W.D. Loehle, D.C. Allbee: *Synth. Met.* **66**, 301 (1994)
14. R. Srinivasan, R.R. Hall, W.D. Wilson, W.D. Loehle, D.C. Allbee: *J. Appl. Phys.* **78**, 4881 (1995)
15. S. Buck: *Polymer* **6**, 319 (1965)
16. A. Brezini, N. Zekri: *J. Appl. Phys.* **75**, 2015 (1994)
17. F. Kokai, H. Saito, T. Fujioka: *J. Appl. Phys.* **66**, 3252 (1989)
18. C. Johnson, J. Mao, S.L. Wunder: In *Polyimides*, Proceeding of the Third International Conference on Polyimides (Ellenville, New York 1988) pp. 70–73
19. I. Savatinova, S. Tonchev, R. Todorov, E. Venkova, E. Liarokapis, E. Anastassakis: *J. Appl. Phys.* **67**, 2051 (1990)
20. D.S. Knight, W.B. White: *J. Mater. Res.* **4**, 385 (1989)